JOC Article

Simple Diastereoselectivity of the $BF_3 \cdot OEt_2$-Catalyzed Vinylogous Mukaiyama Aldol Reaction of 2-(Trimethylsiloxy)furans with Aldehydes

Carlos Silva López, Rosana Álvarez, Belén Vaz, Olalla Nieto Faza, and Ángel R. de Lera*

Departamento de Química Orgánica, Universidade de Vigo, Lagoas-Marcosende, 36310 Vigo, Galicia, Spain

qolera@uvigo.es

Received January 21, 2005

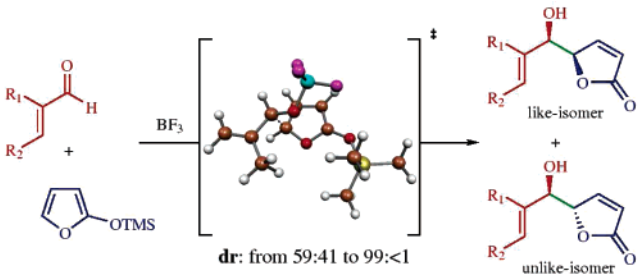

A comprehensive scan of the transition state space for the reaction of 2-(trimethylsiloxy)furan and methacrolein (24 combinations) offered a satisfactory explanation of the high *like* diastereoselectivity obtained experimentally in the Mukaiyama vinylogous aldol reaction of these and related partners. It was determined that the *syn*-γ-hydroxyalkylbutenolides are formed preferentially following a g^+ orientation of the two reactants with the aldehyde in the *s-trans* conformation. Diastereoselectivity is shown to be caused by a combination of subtle effects favoring the formation of the *like* product.

1. Introduction

The Lewis acid-promoted condensation of trialkylsilyl enol-ethers with carbonyl compounds to produce cross-aldol products was reported by Mukaiyama and co-workers in 1974.[1] Synthetically appealing features of these so-called latent enolate aldol reactions are their regioselectivity (reaction at the C_α-position), the great variety of carbonyl compounds or their masked forms that can be used as partners[2] often displaying chemoselectivity (acetals, ketals, ortho esters, and aminoacetals), and the diastereoselectivity derived from the use of a scope of catalysts, promoters, or additives. Recent developments have focused on the enantiocontrol of the process through incorporation of enantiopure ligands on the Lewis acid. All of these features have contributed to the promotion of the Mukaiyama aldol reaction to its present status as a powerful C−C bond-forming process.[3]

As a general trend, *O*-silylated dienolates (extended enolates) derived from both cyclic and acyclic α,β-unsaturated carbonyl compounds react at the γ-position,[4,5] although exceptions are known.[6] The vinylogous aldol[7] reaction has the interest of the synthetic community because of the increased complexity of the δ-hydroxy-α,β-unsaturated carbonyl adduct, with two stereocenters and a stereogenic double bond, relative to the aldol counterpart.

2-(Trimethylsiloxy)furan **1a**, the prototype of the conformationally constrained extended enolates, exhibits the general reactivity pattern for its Lewis acid-induced condensation with aldehydes, ketones, and acetals to produce butenolides,[8] a common scaffold in natural products. Butyrolactones (annonaceous acetogenins)[9] and unsaturated derivatives (γ-alkylidenebutenolides,[10] such as vitamin C and pulvinic acids) are well-known members of this group.

Interestingly, the corresponding lithium dienolate, generated upon treatment of the precursor butenolide

* To whom correspondence should be addressed. Fax: 34986812556.

(1) Mukaiyama, T.; Banno, K.; Narasaka, K. *J. Am. Chem. Soc.* **1974**, *96*, 7503−7509.
(2) Mukaiyama, T.; Ishida, A. *Chem. Lett.* **1975**, *6*, 527−530.
(3) Nelson, S. G. *Tetrahedron: Asymmetry* **1998**, *9*, 357−389.
(4) Mukaiyama, T.; Ishida, A. *Chem. Lett.* **1975**, *4*, 319−322.
(5) Mukaiyama, T.; Ishida, A. *Chem. Lett.* **1975**, *11*, 1201−1202.
(6) Fleming, I.; Lee, T. V. *Tetrahedron Lett.* **1981**, *22*, 705−708.
(7) Casiraghi, G.; Zanardi, F. *Chem. Rev.* **2000**, *100*, 1929−1972.
(8) Asaoka, M.; Yanagida, N.; Ishibashi, K.; Takei, H. *Tetrahedron Lett.* **1981**, *22*, 4269−4270.
(9) Figadère, B. *Acc. Chem. Res.* **1995**, *28*, 359−365.
(10) Brückner, R. *J. Chem. Soc., Chem. Commun.* **2001**, 141−152.

10.1021/jo0501339 CCC: $30.25
Published on Web 03/29/2005

TABLE 1. Experimental Results of the $BF_3{\cdot}OEt_2$-Catalyzed Vinylogous Mukaiyama Aldol Reaction between 2-(Trimethylsiloxy)furans 1a−c and Aldehydes[a]

siloxyfuran	aldehyde	*l*:*u* ratio	yield (%)	ref
1a	**2a**	72:28	40	15
1a	**2b**	78:22	69	15
1a	**2c**	81:19	95	15
1a	**2d**	81:19	95	14
1b	**2e**	88:12	80	16
1a	**2f**	59:41	45	15
1a	**2g**	>99:<1	54	15
1b	**2g**	>99:<1	56	15
1c	**2g**	>99:<1	46	15

[a] Reaction conditions may be found in the appropriate references (see Figure 1).

[2(5*H*)-furanone] with LDA, produced mixtures (ca. 3:1) of α- and γ-adducts with aliphatic aldehydes.[11] In contrast to the stereorandom nature of the adducts derived from the lithium dienolates (ca. 1:1 mixture of the *l*/*u* aldols),[11] the simple diastereoselectivity in the reactions of 2-(trimethylsiloxy)furan **1a** and aldehydes under catalysis by different Lewis acids ranges from moderate to good which produces a mixture of γ-hydroxyalkylbutenolides favoring the like diastereomer.[11−14] For the reaction of **1a** with saturated and unsaturated aldehydes **2a**−**g** promoted by $BF_3{\cdot}OEt_2$, listed in Table 1 (entries 1−6), *l*/*u* ratios range from 59:41 to 81:19. Virtually complete like diastereoselectivity (>99:<1) has been reported for the reaction of 2-(trimethylsiloxy)furan **1a** and the methyl-substituted analogues (**1b**, **c**) with (*E*)-β-iodomethacrolein **2g** (Table 1, entries 7−9).[15]

2. Results and Discussion

In our studies on the total synthesis of carotenoid butenolides,[17] we confirmed the high diastereoselectivity and measured a 91:9 *l*/*u*[18] ratio for the γ-hydroxyalkylbutenolides **3g** formed in the reaction of 3-bromo-2-(trimethylsiloxy)furan **1d** with the same aldehyde **2g** under identical reaction conditions ($BF_3{\cdot}OEt_2$, CH_2Cl_2, −78 °C). To confirm the generality of the outcome, a series of unsaturated aldehydes were surveyed (see Figure 2). The results of their vinylogous Mukaiyama aldol reaction with **1d** are shown in Table 2. Because of the instability of 3-bromo-2-(trimethylsiloxy)furan **1d**, a one-pot condensation reaction involving treatment of 3-bromobutenolide[8] with Et_3N and TMSCl at 25 °C followed by addition of the aldehyde (**2f**−**m**) and the Lewis acid at −78 °C was required. Workup and careful purification by column chromatography and HPLC allowed us to separate the diastereomers **3f**−**m**. The structure of the major product in entry 2 was confirmed as *l*-**3g** (*syn*-**3g**) by means of X-ray crystallography. The major components of the reaction mixtures in entries 1 and 3−7 were assigned as the like[18] aldols by comparison of their ^1H NMR spectra with those of *l*-**3g**. The chemical shifts of $H_{1'}$, found downfield in the *u*-isomer relative to the same signals for the *l*-isomer, are of diagnostic value (differences between 0.13 and 0.60 ppm). Conversely, signals for the γ-butyrolactone H_5 proton are in all cases found downfield in the *l*-isomers, but the difference is not significant (0.02−0.04 ppm).

Analysis of the diastereoselectivity ratios reveals the role of the methyl group at the α-position of the unsaturated aldehyde in the degree of diastereoselectivity of the vinylogous Mukaiyama aldol reaction. Pairwise comparison of entries 1 and 3 and 4 and 7 clearly illustrates the gain in diastereoselectivity imparted by the α-methyl group in **2h** and **2i** relative to **2f** and **2m**, respectively. Only one butenolide was isolated from the reaction of **1d**

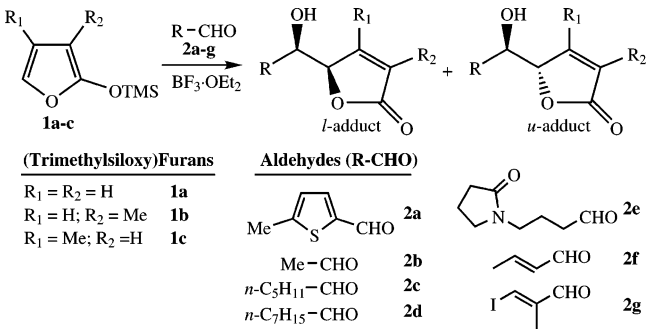

FIGURE 1. Precedents of the vinylogous Mukaiyama aldol reaction of (trimethylsiloxy)furans and achiral aldehydes (Table 1).

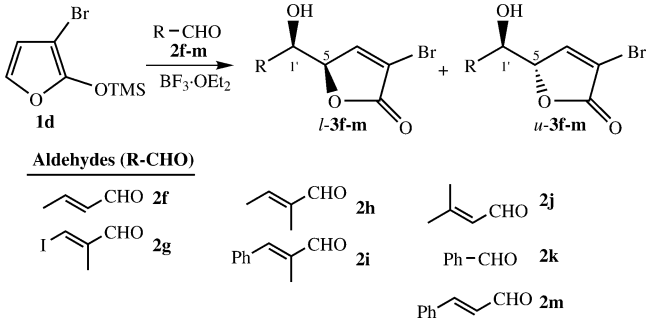

FIGURE 2. Vinylogous Mukaiyama aldol reactions of 3-bromo-2-(trimethylsiloxy)furan **1d** and aldehydes **2f**−**m** catalyzed by $BF_3{\cdot}OEt_2$ (Table 2).

TABLE 2. Experimental Results of the Mukaiyama Reaction between 3-Bromo-2-(trimethylsiloxy)furan 1d and Aldehydes[a]

entry	aldehyde	*l*:*u* ratio	yield (%)
1	**2f**	60:40	68
2	**2g**	91:9	86
3	**2h**	89:11	65
4	**2i**	91:9	74
5	**2j**	80:20	65
6	**2k**	>99:<1	72
7	**2m**	67:33	88

[a] For a pictogram of the reactants involved in each entry see Figure 2.

(11) Brown, D. W.; Campbell, M. M.; Taylor, A. P.; an Zhang, X. *Tetrahedron Lett.* **1987**, *28*, 985−988.
(12) Jefford, C. W.; Jaggi, D.; Boukouvalas, J. *Tetrahedron Lett.* **1987**, *28*, 4037−4040.
(13) Jefford, C. W.; Jaggi, D.; Boukouvalas, J. *Tetrahedron Lett.* **1987**, *28*, 4041−4044.
(14) Szlosek, M.; Franck, X.; Figadère, B.; Cavé, A. *J. Org. Chem.* **1998**, *63*, 5169−5172.
(15) von der Ohe, F.; Brückner, R. *New J. Chem.* **2000**, *24*, 659−669.
(16) Takayama, H.; Kuwajima, T.; Kitajima, M.; Nonato, M. G.; Aimi, N. *Heterocycles* **1999**, *50*, 75−78.
(17) Vaz, B.; Álvarez, R.; Brückner, R.; de Lera, A. R. *Org. Lett.* **2005**, *7*, 545−548.
(18) Seebach, D.; Prelog, V. *Angew. Chem., Int. Ed. Engl.* **1982**, *21*, 654−660.

with benzaldehyde **2k**, which was assigned as the major *l*-**3k**, in keeping with the outcome of the entire series. DFT calculations on the conformational preference of acrolein and its α-methyl analogue provide further insight into this trend (vide infra).

Because the vinylogous Mukaiyama aldol reaction is conducted at −78 °C, high diastereoselectivity can be achieved with very small differences in the activation barriers leading to diastereomers (i.e., a product ratio of 93:7 is expected at −78 °C with only 1 kcal/mol difference in the activation barriers). These small differences in transition state energies, which might drive the reaction through stereodivergent pathways, could be the result of minor changes (even of a conformational nature) in any of the interacting partners. To avoid neglecting any of these prospective determinant effects, we carried out a careful inspection of the potential energy surface of the C−C bond-forming step taking into account all the relevant geometries of both reactants in discrete staggered conformations in an attempt to provide a meaningful description of the reaction stereoselectivity.

For any of these three conformers, the siloxyfuran and the unsaturated aldehyde can approach each other in two nonequivalent orientations; this face selectivity of the C−C bond formation is indicated with the *like* and *unlike* (*lk* and *ul*)[18] descriptors. The alternative antiperiplanar (ap) and synperiplanar (sp) orientations of the OTMS group on the furane and the *s-cis*/*s-trans* conformations of the unsaturated aldehyde have also been taken into consideration. To address the latter, we made the assumption that the lower stability of the *s-trans* conformer of the reactant does not necessarily hold for the transition states where the starting carbonyl is geometrically distorted and other factors, such as the steric interactions with bulky groups, come into play. Because the *trans*-η^1-complex is the most stable adduct formed by an aldehyde and a Lewis acid,[19] it was used as the reference structure for the computations of activation barriers. Altogether, thorough evaluation of the reaction manifold requires that computations for the 24 possible nonequivalent transition structures be made. Table 3 lists the activation energies and C−C bond-forming distances for 22 of them. Two transition structures (labeled g^--ap for the *s-cis* and *s-trans* aldehydes) were not located.[20] Examination of the activation energy values collected in Table 3 leads to the following general conclusions:

(1) The *gauche*$^+$ (g^+) conformers of the forming bond are the lowest in energy of the three rotamers.[21] Differences of 0.53−4.72 kcal/mol are obtained for each conformation of the siloxy group and the unsaturated aldehyde (see relative free energies, $\Delta G^{\ddagger}_{rel}$, Table 3).

(2) Transition states with *s-trans* conformations of the aldehyde moiety show lower energy values than the corresponding *s-cis* structures if all other descriptors are equal.

(3) The orientation of the bulky silyl group affects the relative conformational stabilities of the rotamers. In general, for the series of staggered conformations, an antiperiplanar (ap) disposition of the TMS group slightly favors ap over g^- conformers; the reverse is true for the synperiplanar (sp) conformation of the same bond (see Table 3, relative energies). Nevertheless, with both conformers being disfavored relative to g^+, the influence of the TMS positioning does not significantly affect the stereochemical outcome of the reaction.

(4) The length of the incipient bond also correlates with the above-mentioned trends (see Table 3). The lower-lying g^+ transition states have noticeably longer bonds (earlier transition states) on each series, whereas the less favored structures have 0.14 Å, on average, shorter bond lengths.

(5) Starting from the g^+ relative orientation of the reactants, the *lk* face selectivity presents two available reaction channels with activation energies below 16 kcal/mol (15.33 and 15.60 kcal/mol for g^+-ap and g^+-sp, respectively, in the *s-trans* aldehyde conformation), whereas there is only one channel for the alternative *ul* (g^+-*sp* with 15.57 kcal/mol). This difference, alone, accounts for most of the experimentally determined *like* stereoselectivity.

At the outset, we thought that the factors determining the *like* diastereoselectivity would manifest themselves upon examination of the comprehensive potential energy surface scan (Table 3). However, no rationale has yet emerged, and we came to suspect that a confluence of steric and electronic effects were at play in this reaction. Previous theoretical studies on a related reaction have been reported.[22] The *u* diastereoselectivity in the reaction of 5-alkoxyoxazoles (Figure 3) and aldehydes catalyzed by $AlCl_3$ (the first step preceding the ring opening/ring closing Diels−Alder cascade to 2-oxazolines) was thought to come from an oxygen−oxygen lone pair destabilizing interaction which disfavors the *lk* approach over the *ul*. This explanation does not comply with our experimental and computational results (see Table 3).

To trace the possible sources of this reversal in the facial selectivity, we modeled the reaction of 2-methoxyfuran (isoelectronic of 5-methoxyoxazole) and acetaldehyde using the same level of theory (6-31G*).[22] To complement the study, we considered the consequences of changing not only the facial approach but also the Ar−O−Me conformation (Figure 3). The relative free energies (298 K) of **mod-1a**, **mod-1b**, **mod-1c**, and **mod-1d** reveal that in the 2-methoxyfuran and acetaldehyde reaction the oxygen−oxygen lone pair destabilizing interaction does not govern the course of the reaction. In fact, the structures displaying such an interaction are the lowest in energy (**mod-1a**, 0.0 kcal/mol; **mod-1b**, 1.26 kcal/mol; **mod-1c**, 2.60 kcal/mol; and **mod-1d**, 3.97 kcal/mol). The activation barriers correlate with the dipole moments (**mod-1a**, 8.3 D; **mod-1b**, 8.5 D; **mod-1c**, 8.9 D; and **mod-1d**, 10.3 D) indicating that electronic effects play an important role in the reaction. This hypothesis is also supported by the fact that charge separation is developed along the reaction coordinate, and thus the conformation accommodating more efficiently the charge separation

(19) Santelli, M.; Pons, J.-M. *Lewis Acids and Selectivity in Organic Synthesis;* CRC Press: Boca Raton, FL, 1996.

(20) Analysis of the trends in energy values (Table 3) led us to consider these two transition states very high in energy, and therefore their existence should not alter the conclusions drawn.

(21) The g^+ conformer has been called elsewhere "Diels−Alder-like". This transition state was considered to be favored under Lewis acid catalysis yielding the *like* (*syn*) aldol because of "favourable orbital interactions". In contrast, the alternative, termed "open-chain" (ap in our convention), transition state would be of lower energy under fluoride catalysis because the negative charge would be sparser. For a full discussion see ref 7.

(22) Yu, Z.-X.; Wu, Y.-D. *J. Org. Chem.* **2003**, *68*, 421−432.

TABLE 3. B3LYP/6-311+G(2d,p)//B3LYP/6-31+G(d) Activation Free Energy Barriers for the Vinylogous Mukaiyama Aldol Reaction of 2-(Trimethylsiloxy)furan and Methacrolein[a]

***s-cis*-aldehyde**								
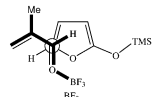	*g*$^-$–*ap*	—	—	—	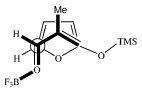	*g*$^-$–*ap*	22.43	4.25	1.92
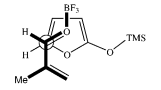	*g*$^+$–*ap*	16.24	0.00	2.13	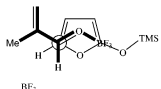	*g*$^+$–*ap*	18.18	0.00	2.13
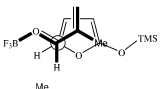	*ap*–*ap*	20.96	4.72	1.98	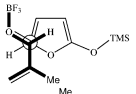	*ap*–*ap*	20.14	1.96	2.01
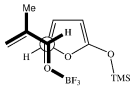	*g*$^-$–*sp*	18.58	2.31	2.14	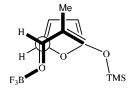	*g*$^-$–*sp*	18.80	1.92	1.99
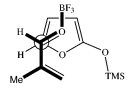	*g*$^+$–*sp*	16.27	0.00	2.16	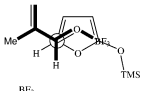	*g*$^+$–*sp*	16.88	0.00	2.20
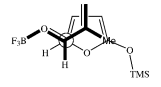	*ap*–*sp*	19.95	3.68	2.02	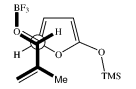	*ap*–*sp*	19.69	2.81	2.02
***s-trans*-aldehyde**								
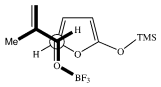	*g*$^-$–*ap*	—	—	—	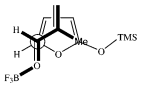	*g*$^-$–*ap*	20.91	4.02	1.87
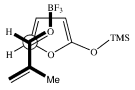	***g*$^+$–*ap***	**15.33**	**0.00**	**2.09**	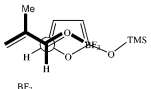	*g*$^+$–*ap*	16.89	0.00	2.07
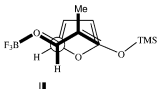	*ap*–*ap*	18.06	2.73	1.93	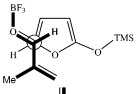	*ap*–*ap*	18.54	1.65	1.99
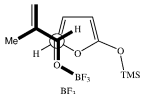	*g*$^-$–*sp*	17.28	1.68	2.10	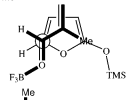	*g*$^-$–*sp*	16.10	0.53	1.93
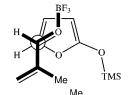	***g*$^+$–*sp***	**15.60**	**0.00**	**2.11**	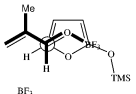	***g*$^+$–*sp***	**15.57**	**0.00**	**2.14**
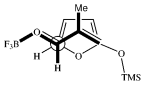	*ap*–*sp*	16.55	0.95	1.96	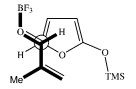	*ap*–*sp*	17.52	1.95	2.03

[a] Geometrical representations are based on ideal rotamers, and they do not represent actual dihedrals. Free energy values (kcal/mol) were computed at 195.15 K. Lengths of the forming bond are provided in Å. Each isomer is denoted as two hyphenated stereochemical descriptors; the first one is related to the rotational isomer of the incipient C−C bond, and the second one is related to the rotational isomer of the silyl ether. $\Delta G^{\ddagger}_{rel}$ values represent the stabilities of rotational isomers relative to the most stable rotamer of the triad. Note that the *lk* approaches are represented in the left column while the *ul* approaches are collected in the right one. Also notice that the *s-cis*/*s-trans* conformers of the aldehyde moiety are vertically separated. Correlations, therefore, occur in columns (*lk* vs *ul*) and rows (*s-cis vs s-trans*).

(lower dipole moment) will be less disfavored. However, steric effects should not be discarded since changing the Ar−O−Me conformation clearly shifts the relative energy of otherwise similar transition states (the sp conformation being 1.26 and 1.37 kcal/mol more stable than the ap counterpart).

The analysis of these two simple models shows that the course of the vinylogous Mukaiyama aldol reaction is dictated by the concomitant effects of both electronic and steric factors. Further inspection of Table 3 also supports the fact that the reaction incorporates an intricate conjunction of effects of different natures; this is confirmed by the lack of trends or correlations in the energy values upon systematic geometrical changes at the transition structures.

The experimental results in Tables 1 and 2 suggest that the presence of a methyl substituent at the α-position of the aldehyde greatly enhances the diastereoselectivity of the vinylogous Mukaiyama aldol reaction. This methyl group has a considerabe effect on the rotational equilibrium of the aldehyde moiety. The *s-cis*/*s-trans* energy difference was calculated at the B3LYP/6-31+G(d) level of theory for acrolein and methacrolein, resulting in values of 1.88 and 3.07 kcal/mol, respectively. Thus, the presence of a methyl group at the α-position widens the energy gap between the *s-cis* and *s-trans* manifold of transition structures which draws the former group out of the competitive process. For α-unsubstituted aldehydes a higher number of transition structures may come into competition, greatly increasing the number of

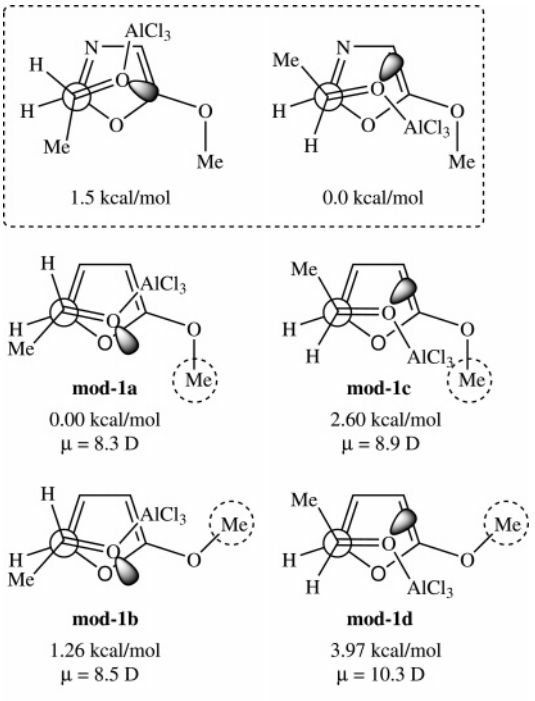

FIGURE 3. Model proposed to predict face selectivity in the reaction of 5-alkoxyoxazoles and aldehydes (dashed box)[22] catalyzed by $AlCl_3$ and a simple model for the isolectronic vinylogous aldol reaction. In addition to transition states **mod-1a** and **mod-1c**, an additional geometrical variation (**mod-1b** and **mod-1d**) involving the Ar−O−Me conformational change was considered.

energetically available (diastereodivergent) pathways and leading to reduced diastereoselectivity.

2.1. Conclusion. In summary, the vinylogous Mukaiyama aldol reaction is fairly sensitive to steric and electronic effects leading to very small differences in the activation barriers of stereodivergent pathways. Nevertheless, high diastereoselectivity is expected because of the low temperature at which the reaction is performed. Despite the fact that the steric and electronic effects involved seem to be highly coupled and, thus, extraction of meaningful and monovariant cause-effect relationships is difficult, some general trends are observed upon thorough inspection of the transition state hypersurface in model systems. The most favorable rotational isomer along the course of the reaction is g^+ for all possible approaches, and this, in combination with the *s-trans* conformation of the aldehyde, leads to the most favorable reaction channels yielding the *l*-diastereomer. The reaction sensitivity to steric effects at the α-position of the unsaturated aldehyde can also be tracked down computationally and experimentally through inclusion of a methyl substituent at such a position.

3. Methods

3.1. Computational Methods. To shed light on the structural reasons for the high *like* diastereoselectivity, we performed DFT computations on model systems involving 2-(trimethylsiloxy)furan **1a** and methacrolein. Electronic structure calculations were performed using the Kohn−Sham formulation of the density functional theory (DFT) with the hybrid exchange functional of Becke[23,24] and the Lee, Yang, and Parr correlation functional[25] (B3LYP). Energy minimum and transition state geometry optimizations were performed in redundant internal coordinates.[26] Harmonic analysis was performed to establish the nature of all stationary points and to allow for evaluation of thermodynamic quantities.

The geometry optimization and frequency calculations were performed using the 6-31+G(d) basis set. Electronic energies and other properties of the density were further refined via single-point calculations at the optimized geometries using the 6-311+G(2d,p) basis set and the B3LYP hybrid density functional. This combination of high-level electronic energy calculations on the optimized geometries obtained at a lower cost is designated by the abbreviated notation B3LYP/6-311+G(2d,p)//B3LYP/6-31+G(d). To ensure high precision for properties sensitive to the use of diffuse basis functions, single-point calculations were run with convergence criteria on the density matrix tightened to 10^{-8} au at each SCF cycle.[27] The selection of the basis functions has been guided by the need to obtain accurate electronic energies while maintaining affordability and balancing size and computational effort.[28] The B3LYP/6-31G(d) theory level was employed with the models **mod-1a**−**d** to allow comparability with previous studies.[22]

All density functional calculations were performed with the Gaussian03[29] suite of programs. Thermodynamic properties at 195.15 K were obtained from the density functional calculations using the standard statistical mechanical expressions for separable vibrational, rotational, and translational contributions within the harmonic oscillator, rigid rotor, and ideal gas/particle-in-a-box models in the canonical ensemble.[30] The standard state in the gas phase is for 1 mol of particles at 298.15 K and 1 atm of pressure.

3.2. Experimental Methods. General Procedure for the Vinylogous Mukaiyama Aldol Reaction. Freshly distilled (2×) chlorotrimethylsilane (0.11 mL, 0.835 mmol, 1.7 equiv) and Et_3N (0.24 mL, 1.67 mmol, 3.4 equiv) were sequentially added dropwise to a solution of 3-bromo-5H-furan-2-one (0.08 g, 0.491 mmol) in CH_2Cl_2 (1 mL). The reaction mixture was stirred for 1 h at room temperature and concentrated under vacuum.

Freshly distilled $BF_3{\cdot}OEt_2$ (0.061 mL, 0.491 mmol, 1 equiv) was added to a cooled (−78 °C) solution of (*E*)-but-2-enal **2f** (0.034 g, 0.491 mmol, 1 equiv) in CH_2Cl_2 (2 mL). To this was added the solution prepared above in CH_2Cl_2 (1 mL) via cannula. After the mixture was stirred for 1.5 h at the same temperature, a phosphate buffer solution (pH 7.1, 5 mL) was added. The mixture was extracted with CH_2Cl_2 (3×); the combined organic layers were dried (Na_2SO_4), and the solvent was removed. The residue was purified by chromatography (silica gel, 80:20:10 hexane/EtOAc/CH_2Cl_2) to produce a mixture of diastereomers which were separated by HPLC (Spherisorb, 5 μm, 25 × 1 cm, 80:20 hexane/EtOAc, 0.6 mL/min) to produce 0.063 g (80%) of (5*R**,1′*R**,2′*E*)-3-bromo-5-(1-hydroxy-2-methylbut-2-enyl)-5*H*-furan-2-one *l*-**3f** and 0.016 g (13%) of the corresponding (5*S**,1′*R**,2′*E*)-3-bromo-5-(1-hydroxy-2-methylbut-2-enyl)-5*H*-furan-2-one *u*-**3f** isomer.

Data for (5*R**,1′*R**,2′*E*)-3-bromo-5-(1-hydroxy-2-methylbut-2-enyl)-5*H*-furan-2-one (*l*-**3f**). ^{1}H NMR (400 MHz, $CDCl_3$): δ 7.46 (s, 1H, H_4), 5.86 (dq, J = 13.1, 6.6 Hz, 1H, $H_{3'}$), 5.46 (ddq, J = 15.3, 7.4, 1.6 Hz, 1H, $H_{2'}$), 4.89 (dd, J = 5.8, 0.9 Hz, 1H, H_5), 4.19 (t, J = 6.4 Hz, 1H, $H_{1'}$), 1.71 (d, J = 1.5 Hz, 3H, CH_3). ^{13}C NMR (100 MHz, $CDCl_3$): δ 168.0 (s, C=O), 149.8 (d), 132.5

(23) Becke, A. D. *Phys. Rev. A* **1988**, *38*, 3098−3100.
(24) Becke, A. D. *J. Chem. Phys.* **1993**, *98*, 5648−5652.
(25) Lee, C.; Yang, W.; Parr, R. G. *Phys. Rev. B* **1988**, *37*, 785−789.
(26) Peng, C.; Ayala, P. Y.; Schlegel, H. B.; Frisch, M. J. *J. Comput. Chem.* **1996**, *17*, 49−56.
(27) Frisch, Æ.; Frisch, M. J. *Gaussian 98 User's Reference*, 2nd ed.; Gaussian, Inc.: Pittsburgh, PA, 1999.
(28) Foresman, J. B.; Frisch, Æ. *Exploring Chemistry with Electronic Structure Methods*, 2nd ed.; Gaussian, Inc.: Pittsburgh, PA, 1996.
(29) Frisch, M. J.; et al. *Gaussian 03*, revision B.01; Gaussian, Inc.: Pittsburgh, PA, 2003.
(30) Cramer, C. J. *Essentials of Computational Chemistry: Theories and Models;* John Wiley & Sons: Chichester, England, 2002.

(d), 126.8 (d), 114.3 (s), 85.0 (d), 73.2 (d), 17.9 (q). MS (ESI^+): *m/z* (%) 257 ($M^+ + 23$, 98), 255 ($M^+ + 23$, 100), 217 (15), 215 (15). HRMS (FAB^+): calcd for $C_8H_9{}^{79}BrNaO_3$, 254.9627; found, 254.9623; calcd for $C_8H_9{}^{81}BrNaO_3$, 256.9607; found, 256.9602.

Data for (5*S**,1′*R**,2′*E*)-3-bromo-5-(1-hydroxy-2-methylbut-2-enyl)-5*H*-furan-2-one (*u*-**3f**). ^1H NMR (400 MHz, $CDCl_3$): δ 7.52 (d, $J = 1.8$ Hz, 1H, H_4), 5.88 (m, 1H, $H_{3'}$), 5.49 (ddq, $J =$ 15.3, 6.5, 1.6 Hz, 1H, $H_{2'}$), 4.87 (dd, $J = 4.8$, 1.8 Hz, 1H, H_5), 4.32 (t, $J = 4.8$ Hz, 1H, $H_{1'}$), 1.74 (m, 3H, CH_3). ^{13}C NMR (100 MHz, $CDCl_3$): δ 168.2 (s, C=O), 149.8 (d), 131.5 (d), 127.2 (d), 114.3 (s), 84.8 (d), 72.2 (d), 17.9 (q). MS (ESI^+): *m/z* (%) 257 ($M^+ + 23$, 98), 255 ($M^+ + 23$, 100), 231 (14), 229 (13), 217 (10), 215 (12). HRMS (FAB^+): calcd for $C_8H_9{}^{79}BrNaO_3$, 254.9627; found, 254.9622; calcd for $C_8H_9{}^{81}BrNaO_3$, 256.9607; found, 256.9602.

Acknowledgment. We thank the European Commission (QLK3-2002-02029, "Anticancer Retinoids"), the Spanish Ministerio de Ciencia y Tecnología (Grant SAF01-3288, Ramón y Cajal Research Contract to R.Á. and FPU fellowships to C.S.L., B.V., and O.N.F.) and Xunta de Galicia (Grant PGIDIT02PXIC30108PN) for financial support. We are also grateful to the Centro de Supercomputación de Galicia (CESGA) for allocation of computing time.

Supporting Information Available: Typical experimental procedures for the synthesis of all compounds, their physical and spectroscopic data, X-ray structural data for compound *l*-**3g** (CIF), and Cartesian coordinates and electronic energies of computed structures. This material is available free of charge via the Internet at http//www.pubs.acs.org.

JO0501339